International Journal of Electrical, Electronic and Communication Sciences
ISSN: 2517-9438
Vol:12, No:11, 2018

DC-Link Voltage Control of DC-DC Boost Converter-Inverter System with PI Controller

Thandar Aung, Tun Lin Naing

***Abstract*—**In this paper, the DC-link voltage control of DC-DC boost converter–inverter system is proposed. The mathematical model is developed from four different sub-circuits that depended on the switch positions. The developed differential equations are combined to develop the dynamic model. Transfer function is generated from the switched function model. Fluctuation of DC-link voltage causes connected loads malfunction. For this problem, a kind of traditional controller, the PI controller is applied to achieve constant DC-link voltage. The PI controller gains are obtained based on transfer function step response. The simulation work has been studied by using MATLAB/Simulink software and hardware prototype is implemented with a low-cost microcontroller Arduino Nano. Experimental results are collected by using ArduinoIO library package. Closed-loop DC-link voltage control system is tested with various line and load disturbances. It is found that the experimental results give equal responses with the simulation results.

***Keywords*—**ArduinoIO library package, boost converter-inverter system, low cost microcontroller, PI controller, switched function model.

I. Introduction

IN recent years, the growing need for more efficient power supplies and power conversion has played a significant role. Various kinds of converters, Buck converter, Boost converter, Buck-Boost converter and Cuk converter are described in [1], [2]. Boost converters are also known as switched mode power supply which produces output voltage higher than that of input voltage. Inverters are form of power converters that convert DC input voltage into AC output voltage. The topology of boost converter–inverter system has a wide range of applications which include renewable energy applications, electric vehicles, telecommunications, many home appliances, industrial and commercial applications, DC motor drive, voltage regulators and so on [3]-[5].

Modeling and theoretical analysis of DC-link voltage control of converter have become an important research topic in modern power electronics. However, boost converters have a non-mi nimum phase problem (initial undershoot) due to the presence of a right-half-plane (RHP) zero in their plant transfer function [6]. It is difficult for the system to show good performances with line perturbations and load variations. For these restrictions, a kind of traditional controller i.e., the PI controller is used to control the DC-link voltage of system to obtain the stable output voltage. In this study, the controller gains of the PI controller are developed based on transfer function step response.

There have been several control methods studied in the literature [6]-[8]. There are a number of classical controllers used in DC-link voltage control such as PI controller, PID controller, fuzzy controller, sliding mode controller and so on [9]-[11]. There also exists special kind of controllers such as Type-II and Type-III controller [12]. In the previous work, many researchers took their effort to voltage mode control of the boost converter. The DC-link voltage control of photovoltaic inverter used in renewable system has been presented in [13]. The dynamic performance of the soft-switched DC-DC converter was improved by using the PI controller which was designed by using frequency response technique and results were simulated using PSIM [14].

Cascade control structure with PI, used to solve undershoot and sluggish dynamic response of boost DC-DC converter, are proposed in [15]. TMS320LF2407 DSP of TI Company is developed for experimental evaluation. Voltage-lift technique is used to obtain higher output voltage. Closed-loop PI control is used to minimize ripple of parasitic elements and hardware prototype, implemented by using DSPTM320F2812 process controller, are presented in [16]. The detailed analysis of open loop control, closed loop current mode and closed loop voltage mode control of boost converter, verified with experimental and simulation results are presented in [17], PI compensator is designed from the study of root locus plot and bode diagram revealed with pole placement method. Mario in [18] proposed DC motor speed control by using Arduino support package and MATLAB Simulink to create control algorithm. In this research, ArduinoIO library package is used to create the model of controller in MATLAB/ Simulink and collect data by serial communication.

The main objective of this paper is to achieve constant DC-link voltage of DC-DC boost converter–inverter system. The general objectives are to implement the system by using low-cost microcontroller and to validate the mathematical model with experimental tests.

The rest of this paper is organized as follows: Modeling and the transfer function of the system are developed in Section II. DC-link voltage control with suitable PI controller gains are presented in Section III. Section IV presents simulation results and discussion. Section V describes experimental results and discussion. Finally, Section VI concludes this research.

II. Modeling and Transfer Function of DC-DC Boost Converter-Inverter System

The DC-link voltage control of two-stage DC-DC boost

Thandar Aung is with the Mandalay Technological University, Mandalay, Myanmar, (e-mail: thandar.aung.epep@gmail.com).
Tun Lin Naing is with the Department of Electrical Power Engineering, Mandalay Technological University, Mandalay, Myanmar, (e-mail: tunlinnaing1980@gmail.com).

converter-inverter system is implemented by using PI controller. The boost converter is DC-DC stage which boosts the input voltage up to DC-link voltage. It consists of inductor L with parasitic resistance r_L, switch Q_1 with control signal $q_1(t)$, diode D and DC-link capacitor C_{dc}. During switch ON, the inductor stores energy. During switch OFF condition, the stored energy appears in series with the input source and supplies the output. The capacitor is used for the filtering of ripple in the output voltage.

The DC-AC conversion stage is also called inverter which converts DC-link output voltage of boost converter into AC output voltage required by the load. It is comprised of four transistors Q_2 and $\overline{Q}_2$ with control signal q_2 and $\bar{q}_2(t)$. Output load resistor R_o is connected with the inverter through the LC output filter (L_f, r_f, C_f).

In order to obtain the output voltage stable and connected loads operate in normal condition, it is needed to control the DC-link voltage of the system at a required voltage level. The control scheme of the system with PI controller is demonstrated in Fig. 1. When the feedback signal obtained from the DC-link voltage is compared with the set reference voltage V_{ref}, the error voltage V_{err} is obtained. This error voltage is applied to the PI controller that defines the duty ratio for the PWM generator which generates a control signal for switch Q_1.

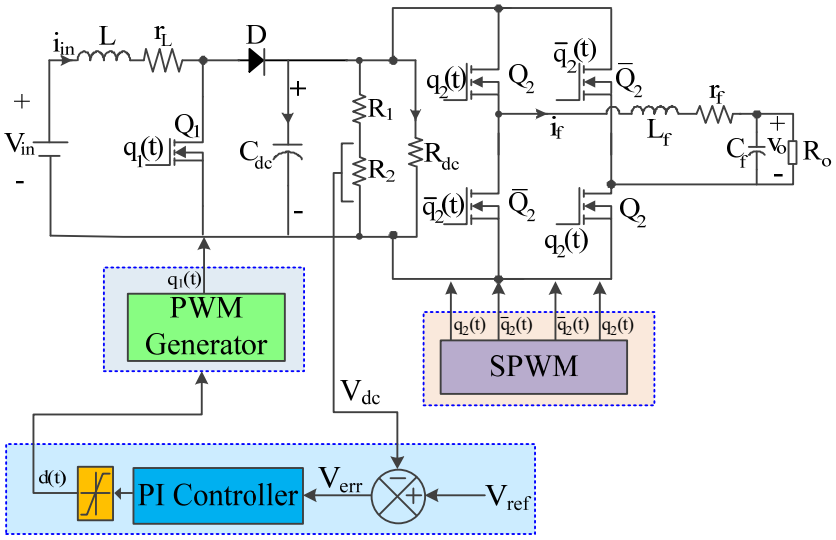

Fig. 1 DC-DC Boost Converter-Inverter System with Control Scheme

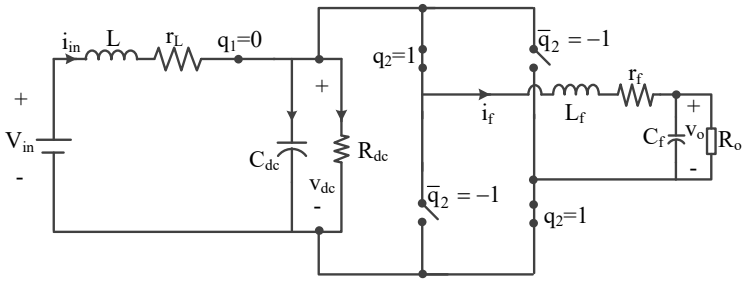

Fig. 2 Equivalent Circuit of Mode 1

A. Circuit Operation of Four Modes

The system has four logics because the control signals of transistors have two ON/OFF conditions (0 or 1). Therefore, the system operates in four modes depending on switch ON/OFF condition. The mathematical models of four modes can be represented by the differential equations. These differential equations are obtained by applying KVL and KCL. The equivalent circuit of four modes are illustrated in Figs. 2-5.

Mode 1: Q_1-OFF and Q_2-ON. Fig. 2 shows the equivalent circuit of $q_1 = 0$ and $q_2 = 1$.

From Fig. 2, differential equations (1)-(4) are obtained:

$$L\frac{di_{in}}{dt} = V_{in} - i_{in}r_L - v_{dc} \quad (1)$$

$$C_{dc}\frac{dv_{dc}}{dt} = i_{in} - i_f - \frac{v_{dc}}{R_{dc}} \quad (2)$$

$$L_f \frac{di_f}{dt} = v_{dc} - i_f r_f - v_o \quad (3)$$

$$C_f \frac{dv_o}{dt} = i_f - \frac{v_o}{R_o} \quad (4)$$

Mode 2: Q_1-OFF and Q_2-OFF. Fig. 3 shows the equivalent circuit of q_1=0 and q_2=-1.

The differential equations of Fig. 3 are represented in (5)-(8):

$$L \frac{di_{in}}{dt} = V_{in} - i_{in} r_L - v_{dc} \quad (5)$$

$$C_{dc} \frac{dv_{dc}}{dt} = i_{in} + i_f - \frac{v_{dc}}{R_{dc}} \quad (6)$$

$$L_f \frac{di_f}{dt} = -v_{dc} - i_f r_f - v_o \quad (7)$$

$$C_f \frac{dv_o}{dt} = i_f - \frac{v_o}{R_o} \quad (8)$$

Mode 3: Q_1-ON and Q_2-ON. Fig. 4 shows the equivalent circuit of q_1=1 and q_2=1.

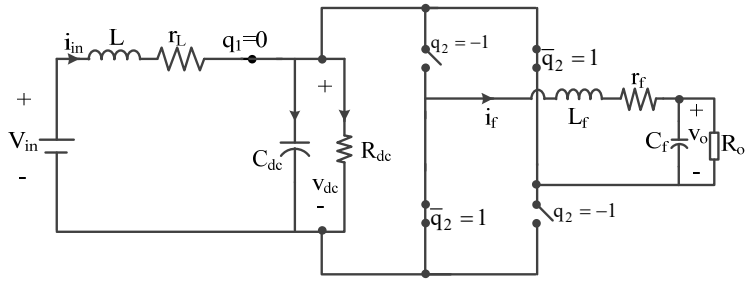

Fig. 3 Equivalent Circuit of Mode 2

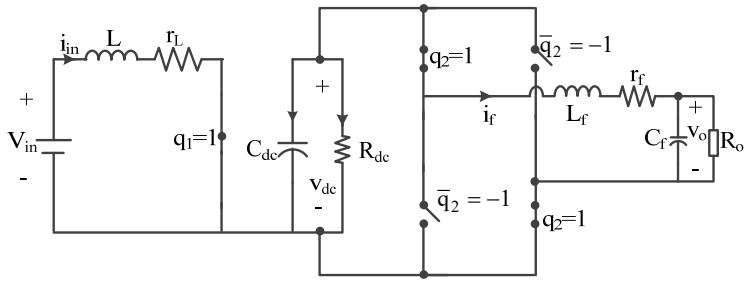

Fig. 4 Equivalent Circuit of Mode 3

The mathematical models of Fig. 4 can be represented by (9)-(12):

$$L \frac{di_{in}}{dt} = V_{in} - i_{in} r_L \quad (9)$$

$$C_{dc} \frac{dv_{dc}}{dt} = -i_f - \frac{v_{dc}}{R_{dc}} \quad (10)$$

$$L_f \frac{di_f}{dt} = v_{dc} - i_f r_f - v_o \quad (11)$$

$$C_f \frac{dv_o}{dt} = i_f - \frac{v_o}{R_o} \quad (12)$$

Mode 4: Q_1-ON and Q_2-OFF. Fig. 5 shows the equivalent circuit of q_1=1 and q_2=-1.

The mathematical models of Fig. 5 are shown in (13)-(16):

$$L \frac{di_{in}}{dt} = V_{in} - i_{in} r_L \quad (13)$$

$$C_{dc} \frac{dv_{dc}}{dt} = i_f - \frac{v_{dc}}{R_{dc}} \quad (14)$$

$$L_f \frac{di_f}{dt} = -v_{dc} - i_f r_f - v_o \quad (15)$$

$$C_f \frac{dv_o}{dt} = i_f - \frac{v_o}{R_o} \quad (16)$$

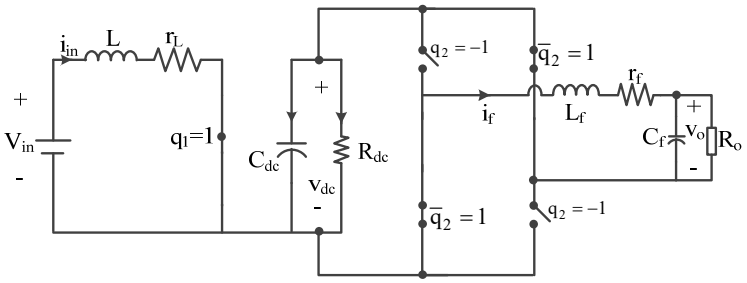

Fig. 5 Equivalent Circuit of Mode 4

TABLE I
PARAMETERS OF THE SYSTEM

Parameters	Variables	Values	Unit
Supply voltage	V_{in}	12	[V]
Switching frequency	f_{boost}	4000	[Hz]
	$f_{inverter}$	11000	[Hz]
Inductor	L	2	[mH]
Inductor resistance	r_L	0.2	[Ω]
DC-link capacitance	C_{dc}	1.41	[mF]
DC-link resistance	R_{dc}	1000	[Ω]
Duty-cycle of boost converter	$D_{1\,(avg)}$	70	[%]
Output filter capacitance	C_f	22	[μF]
Output filter inductance	L_f	2	[mH]
Output filter resistance	r_f	0.2	[Ω]
Load resistance	R_o	22	[Ω]
Inverter Output voltage	V_o	24	[V_{rms}]
Fundamental Inverter output frequency	f	50	[Hz]

B. Switched Model of the System

To obtain the dynamic model of the system, all of these differential equations from four modes are combined by using switching function. $q_1 \in \{0,1\}$ and $q_2 \in \{1,-1\}$ are the input switch positions of transistors Q_1 and Q_2. The switched models of this system can be represented as shown in (17)-(20):

$$L\frac{di_{in}}{dt} = V_{in} - i_{in}r_L - (1-q_1)v_{dc} \tag{17}$$

$$C_{dc}\frac{dv_{dc}}{dt} = (1-q_1)i_{in} - q_2 i_f - \frac{v_{dc}}{R_{dc}} \tag{18}$$

$$L_f\frac{di_f}{dt} = q_2 v_{dc} - i_f r_f - v_o \tag{19}$$

$$C_f\frac{dv_o}{dt} = i_f - \frac{v_o}{R_o} \tag{20}$$

The switch positions q_1 and q_2 are replaced by averaged positions d_1 and d_2 in (17)-(20). The averaged switched models of the system are shown in (21)-(24):

$$\frac{d\bar{i}_{in}}{dt} = \frac{1}{L}\left[V_{in} - \bar{i}_{in}r_L - (1-\bar{d}_1)\bar{v}_{dc}\right] \tag{21}$$

$$\frac{d\bar{v}_{dc}}{dt} = \frac{1}{C_{dc}}\left[(1-\bar{d}_1)\bar{i}_{in} - \bar{d}_2\bar{i}_f - \frac{\bar{v}_{dc}}{R_{dc}}\right] \tag{22}$$

$$\frac{d\bar{i}_f}{dt} = \frac{1}{L_f}\left[\bar{d}_2\bar{v}_{dc} - \bar{i}_f r_f - \bar{v}_o\right] \tag{23}$$

$$\frac{d\bar{v}_o}{dt} = \frac{1}{C_f}\left[\bar{i}_f - \frac{\bar{v}_o}{R_o}\right] \tag{24}$$

By using (21)-(24), changes of system dynamic performances can be easily studied by numerical simulations. The parameters of the components used in this system are displayed in Table I.

C. Transfer Function

The overall system consists of boost converter dynamic parameters and inverter dynamic parameters. It is difficult to obtain overall plant transfer function of the system. In order to ensure system simplicity, the portion of inverter dynamics with output LC filter must be reduced and considered as an output load resistance. Therefore, the transfer function of boost converter becomes the plant transfer function of the system. The reduced system plant transfer function is used to find suitable controller gains. The inverter reduced circuit of the system is obtained as shown in Fig. 6.

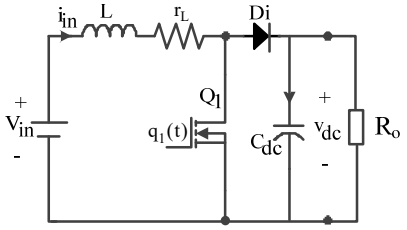

Fig. 6 Reduced Circuit of the System

The control to DC-link voltage transfer function of the system is represented in (25), where D_1 is the average duty cycle of boost converter.

$$\frac{\tilde{v}_{dc}}{\tilde{d}} = \frac{-V_{in}\left[s - \dfrac{R_o(1-D_1)^2 - r_L}{L}\right]}{C_{dc}\left[R_o(1-D_1)^2 + r_L\right]\left[s^2 + s\dfrac{L + r_L R_o C_{dc}}{LR_o C_{dc}} + \dfrac{R_o(1-D_1)^2 + r_L}{LR_o C_{dc}}\right]} \tag{25}$$

The plant transfer function of the system calculated with parameters shown in Table I is

$$G_p(s) = \frac{-12s + 1.068\times10^4}{0.003074s^2 + 0.4065s + 108} \quad (26)$$

According to Fig. 7, it has been obviously found that a right-half plane zero (RHPZ) presents in the transfer function of the system. It causes undesired effects (undershoot) in converter dynamic responses. Fig. 7 illustrates plant transfer function of the system with Bode diagram where gain margin G_m= -29.4dB, phase margin P_m= -75.6˚ and phase crossover frequency W_{pm}= 4.01x10^3 rad/s.

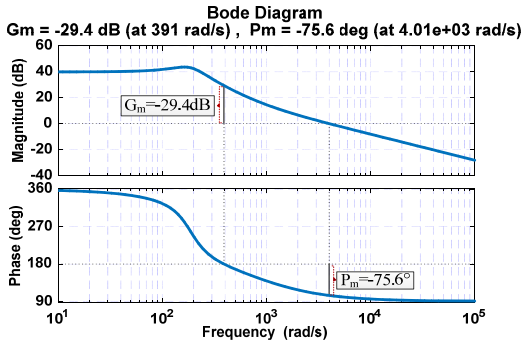

Fig. 7 Plant Transfer Function

III. DC-Link Voltage Control with PI Controller

When DC-link feedback voltage is compared with the reference voltage, an error voltage is obtained. That error voltage is applied to the PI controller to compensate for the error signal. PI controller produces a duty cycle command for PWM generator which provides controlled pulses for the switch Q_1. The closed loop control system with plant and PI controller is shown in Fig. 8.

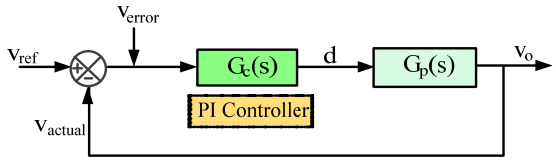

Fig. 8 Block Diagram of Closed-loop Control

The operation of controller plays an important role in obtaining good performance and the regulated output of converters. RHPZ causes undesired effects (undershoot) and these effects cannot be removed but can be reduced with an appropriate controller. The PI controller is used in this paper to reduce RHPZ effects. The PI controller equation is expressed in (27) where ω_L is line frequency. The transfer function of PI controller is described in (28) where k_p is the proportional gain and k_i is the integral gain.

$$G_c(s) = G(\infty)\left(1 + \frac{\omega_L}{s}\right) \quad (27)$$

$$G_c(s) = k_p + \frac{k_i}{s} \quad (28)$$

A. PI Controller Gain

The cut off frequency, f_c is taken as 2% of switching frequency in [19]. In this study, cut off frequency is calculated as 70% of the sampling frequency and ω_L is taken the same as f_c. The sampling frequency of this system is chosen as 500 Hz. Value of ω_L is 2199.11 rad/s and from Fig. 7, gain at 350 Hz is 32 dB.

$$-20\log G(\infty) = 32\text{dB}$$

$$G(\infty)=0.02512$$

The value of $G(\infty)$ and ω_L are known, the transfer function of PI controller is developed.

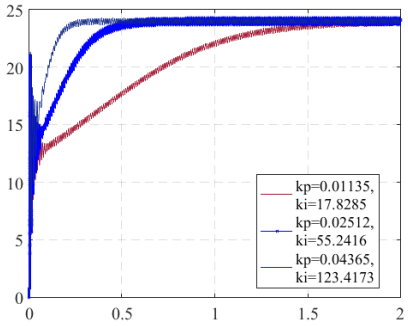

Fig. 9 Step-response of PI Controller with Different k_p, k_i Values

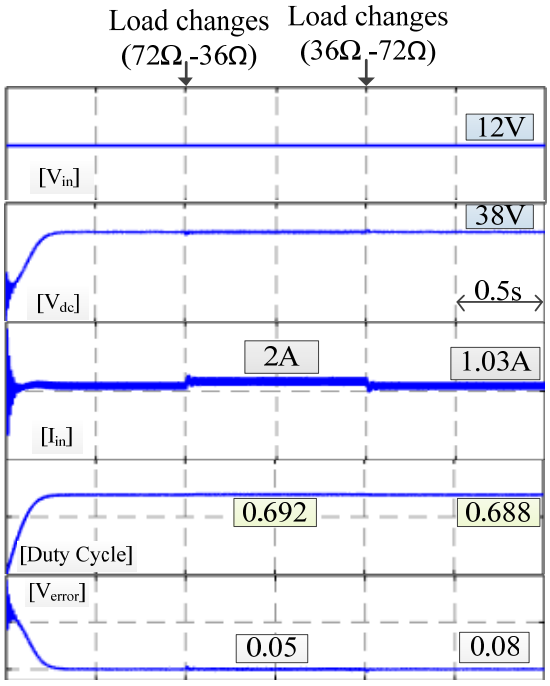

Fig. 10 Simulated Responses of V_{in}, V_{dc}, I_{in} and Duty Cycle with Load Disturbance (72Ω -36Ω -72Ω)

The step response of PI controller with different values of k_p and k_i are plotted in Fig. 9. Among these controller gains, the suitable controller gains are k_p=0.02512 and k_i=55.2416. Other controller gains have slow responses and initial responses have a lot of noises. The transfer function of PI controller used in this research is mentioned in (29):

$$G_c(s) = 0.02512 + \frac{55.2416}{s} \quad (29)$$

IV. Simulation Results

The simulation works are carried out by using MATLAB/ Simulink software. The system is tested with line perturbation and load variations at time 1 s and 2 s are shown in Figs. 10 and 11. The DC-link reference voltage is 38 V.

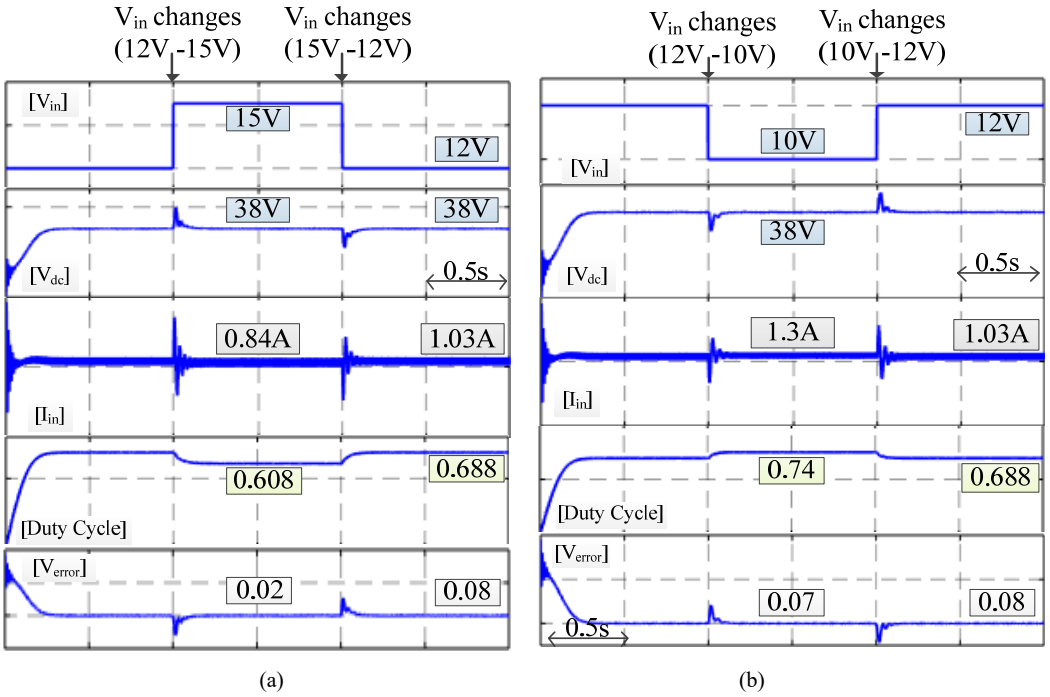

Fig. 11 Simulated Responses of V_{in}, V_{dc}, I_{in} and Duty Cycle with Supply Voltage Change (a) 12V-10V-12V and (b) 12V-15V-12V

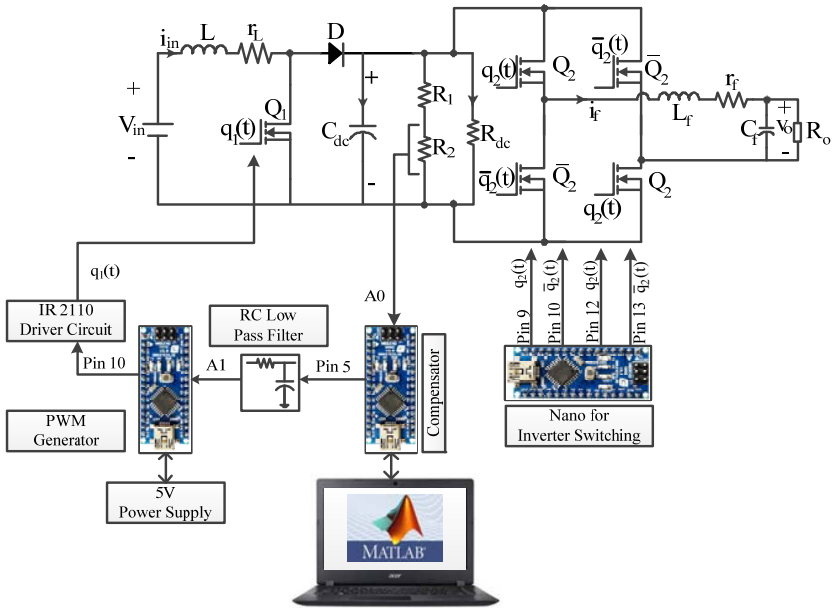

Fig. 12 Hardware Set-up of the System

When load change occurs, DC-link voltage response does not change significantly. Input current and duty-cycle change a little according to load disturbances. When V_{in} decreases, V_{dc} decreases but immediately reaches to its reference value. At that time, I_{in} and duty-cycle increases with respect to changes of V_{in}. When the value of V_{in} increased, V_{dc} has little overshoot and within a few milliseconds it can immediately recover to its reference value, I_{in} and duty-cycle decreases with respect to changes of V_{in}. Zero steady-state error can be seen in these simulation results. The responses of all waveform are smooth in the simulation study.

V. Experimental Results

By using Arduino IO library package, the DC-DC boost converter–inverter system is implemented to determine the performance of PI controller. The hardware set-up of DC-DC boost converter–inverter system with low-cost microcontroller has been implemented in Fig. 12.

The experimental prototype of DC-DC boost converter–inverter system with low cost microcontroller Arduino Nano is illustrated in Fig. 13.

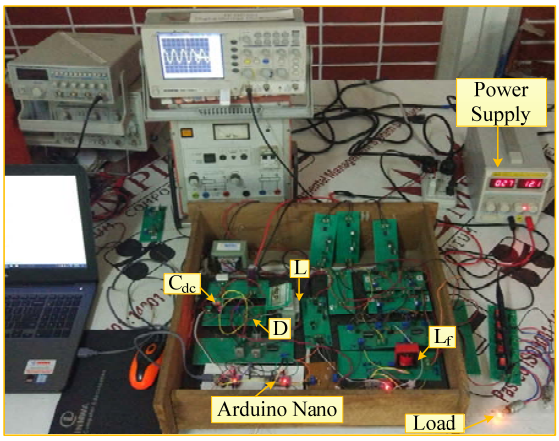

Fig. 13 Experimental Prototype

In this research, ArduinoIO library package is used to interface real time simulation between software and hardware. Simulink block diagram of DC-link voltage control by using ArduinoIO library blocks are demonstrated in Fig. 14.

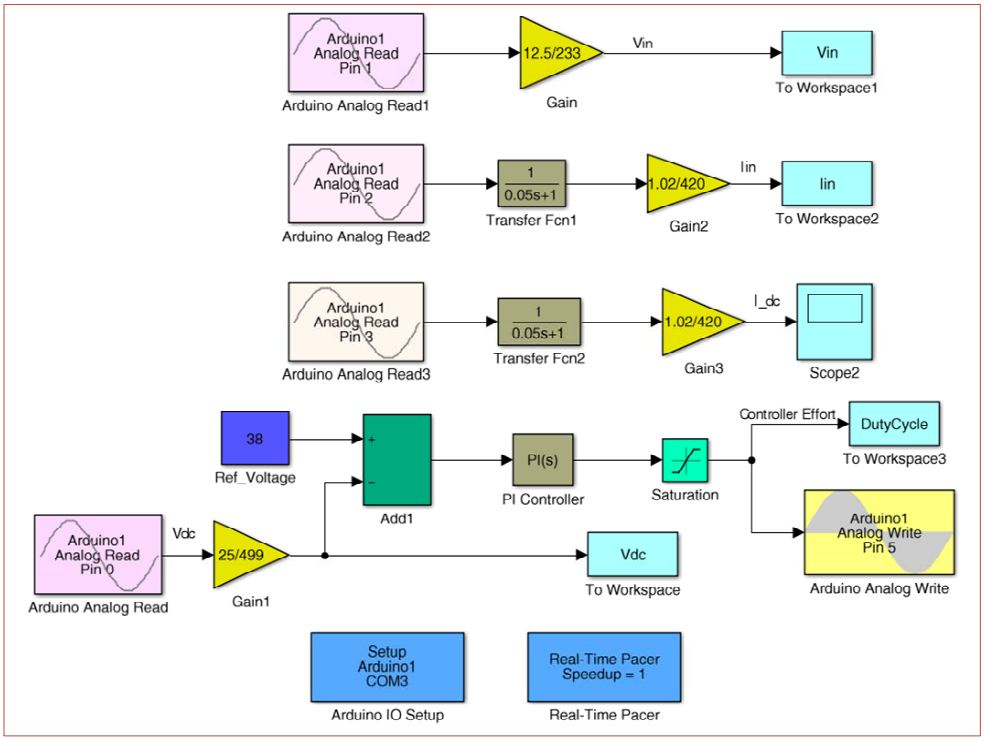

Fig. 14 Simulink Model of Closed-loop Control with ArduinoIO Library Blocks

The experimental tests are carried out the same condition as simulation works. The reference DC-link voltage is also 38 V. The experimental results of closed-loop control during line and load disturbances are shown in Figs. 15 and 16.

When the system undergoes changes, DC-link voltage fluctuated at the moment of changes time. V_{dc} has a little overshoots and undershoots at the time of supply voltage changes. When the system exposes supply voltage changes, V_{dc} has just a little undershoot in the initial condition and V_{dc} reaches to its reference voltage 38 V within a few second. The changes of I_{in} and duty-cycle depend on supply voltage increase or decrease. I_{in} and duty-cycle change a little with respect to variations of load. It can be clearly seen that these experimented responses totally show the same behavior as the

simulated responses.

VI. Conclusion

DC-link voltage control of DC-DC boost converter–inverter system with PI controller has been implemented. Proper PI controller gains are chosen, based on transfer function step-response. It can explicitly be seen that the DC-DC boost converter-inverter system cooperated with PI controller generates stable DC-link voltage when the system undergoes any disturbances. Experimental implementation of hardware prototype based on a low-cost microcontroller is described to validate the simulation results. The obtained results show that the experimental results totally agreed with the simulation results. These facts proved the robustness and effectiveness of DC-link voltage control of the system using the PI controller.

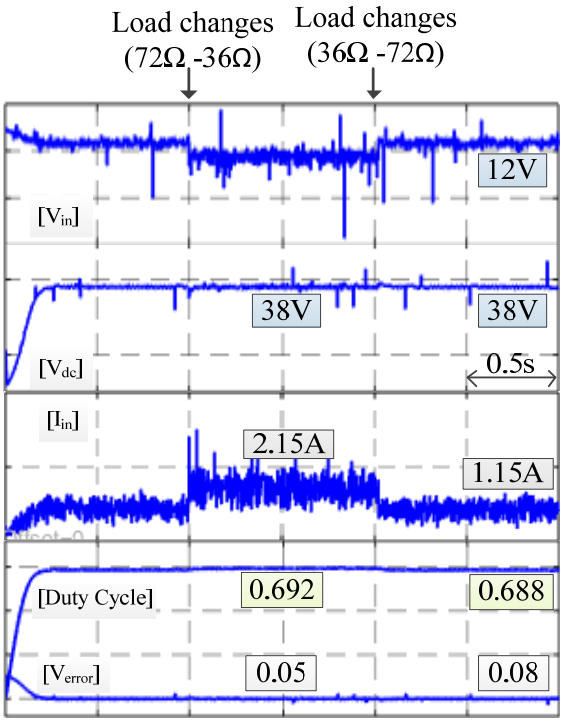

Fig. 15 Experimented Responses of V_{in}, V_{dc}, I_{in} and Duty Cycle with Load Disturbance (72Ω-36 Ω -72 Ω)

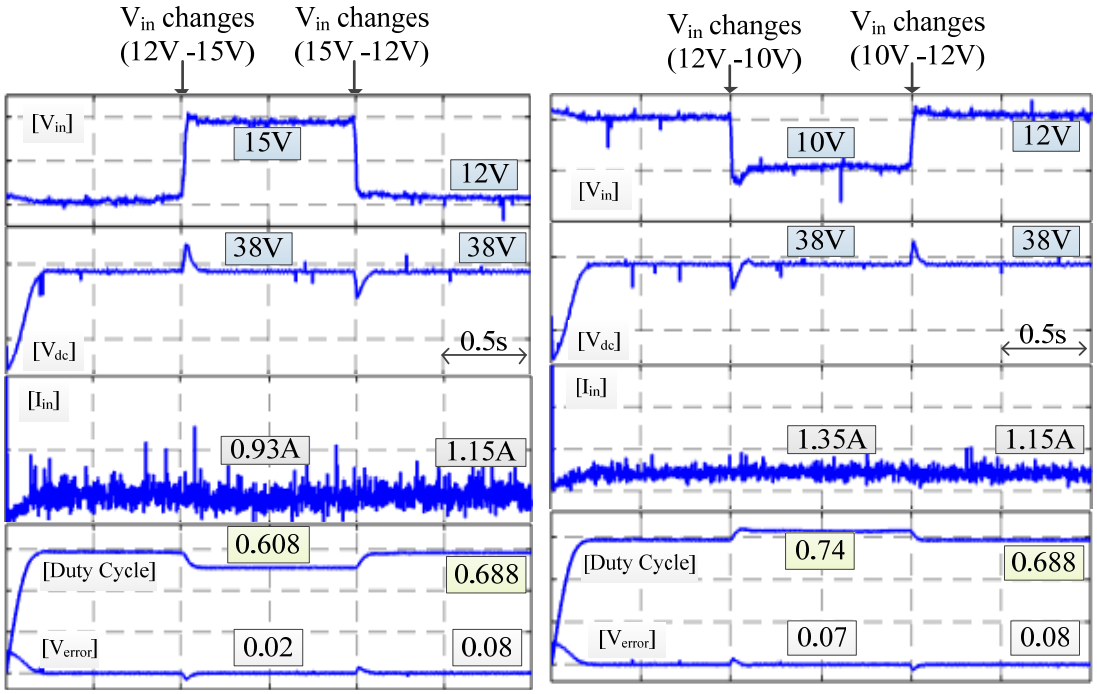

(a) (b)

Fig. 16 Experimented Responses of V_{in}, V_{dc}, I_{in} and Duty Cycle with V_{in} Change (a) 12V-10V-12V and (b) 12V-15V-12V

References

[1] Daniel W. Hart, Power Electronics, 2011, ISBN 978-0-07-3380674.
[2] Juan Manuel Enrique Gomez, Antonio Javier Barragan Pina, Eladio Duran Aranda and Jose Manuel Andujar Marquez, "Theoretical Assessment of DC/DC Power Converters' Basic Topologies. A Common Static Model", *Appl. Sci. 2018*, Aug 19, 2018.
[3] Victor Hugo Garcia-Rodriguez, Ramon Silva-Ortigoza, Eduardo

Hernandez-Marquez, Jose Rafael Garcia-Sanchez, Mario Ponce-Silva and Griselda Saldana-Gonzalez, "A DC Motor Driven by a DC-DC Boost Converter-Inverter: Modeling and Simulation", *2016 International Conference on Mechatronics and Automotive Engineering (ICMEAE)*, Nov. 22-25, 2016, pp. 78-83.

[4] Neng Zhang, Danny Sutanto and Kashem M. Muttaqi, "A Buck-Boost Converter Based Multi-Input DC-DC/AC Converter", *2016 IEEE International Conference on Power System Technology Wollongong NSW,* Sep/Oct. 2016, pp. 1-6.

[5] Xianhao Yu, Qin Lei, and Fang Zheng Peng, "Boost Converter – Inverter System Using PWAM for HEV/EV Motor Drive", *2012 Twenty-Seventh Annual IEEE, Applied Power Electronics Conference and Exposition (APEC)*, 2012, pp. 946-950.

[6] Katsuhiko Ogata, "Modern Control Engineering", 5th Edition, Pearson Electronics, India, 2010.

[7] P. Sanchis, A. Ursua, E. Gubia and L. Marroyo, "Design and experimental operation of a control strategy for the buck–boost DC–AC inverter", *IEEE Proceedings on Electric Power Applications,* vol. 152, ni.3, May 2005, pp. 660-668.

[8] Pablo Sanchis, Alfredo Ursæa, Eugenio Gubia, and Luis Marroyo, "Boost DC–AC Inverter: A New Control Strategy", *IEEE Transactions on Power Electronics*, vol. 20, no. 2, Mar 2005, pp.343-353.

[9] Lopamudra Mitra and Nibedita Swain, "Closed Loop Control of Solar Powered Boost Converter with PID Controller", *2014 IEEE International Conference on Power Electronics, Drives and Energy Systems (PEDES)*, 2014, pp. 1-5.

[10] Arka Bhattacaharya, P. Rja and A. Pavan Kumar, "Modeling and Simulation of a Controlled DC-AC Converter System Using Sliding Mode Controller Mechanism", *2011 International Conference on Process Automation, Control and Computing*, 2011, pp. 1-8.

[11] Liviu Dinca and Jenica-Ileana Corcau, "P.I. Versus Fuzzy Control For A DC to DC Boost Converter", *2016 International Symposium on Power Electronics, Electrical Drives, Automation and Motion (SPEEDAM)*, 2016, pp. 803-808.

[12] Arnab Ghosh and Subrara Banerjee, "Design of Type III Controller for DC-DC Switch Mode Boost Converter", *6th IEEE Power India International Conference (PIICON)*, pp. 1-6, New Dahli, India, 2014.

[13] L. Nousiainen and T. Suntio, "DC-Link Voltage Control of a Single-Phase Photovoltaic Inverter", *6th IET International Conference on Power Electronics, Machines and Drives (PEMD 2012)*, Bristol, U.K, Sep. 2011, pp. 1-6.

[14] X. Felix Joseph, Dr. S. Pushpakumar, D. Arun Dominic and D.M. Mary Synthia Regis Prabha, "Design and Simulation of a Soft Switching Scheme for a DC-DC Boost Converter with PI Controller', *2011 International Conference on Emerging Trends in Electrical and Computer Technology*, 2011, pp. 370 – 374.

[15] Jinbo Liu, Wenlong Ming, Fanghong Gao, "A New Control Strategy for Improving Performance of Boost DC/DC Converter Based on Input-Output Feedback Linearization", *2010 8th World Congress on Intelligent Control and Automation,* 2010, pp. 2439 – 2444.

[16] Sanjeevikumar Padmanaban, Ersan Kabalci, Atif Iqbal, Haitham Abu-Rub and Olorunfemi OjoE, "Control strategy and hardware implementation for DC-DC boost power circuit based on proportional integral compensator for high voltage application", Volume 18, Issue 2, June 2015, pp. 163-170.

[17] Saswati Swapna Dash and Byamakesh Nayak, "Control analysis and experimental verification of a practical dc–dc boost converter", Volume 2, Issue 3, Dec 2015, pp. 378-39.

[18] Mario Gavran, Mato Fruk and Goran Vujisic, "PI Controller for DC Motor Speed Realized with Arduino and Simulink", *IEEE, MIPRO,* May 22-26, pp. 1557-1561, 2017.

[19] Gokhan Altintas, Mehmet Onur Gulbahce and Derya Ahmet Kocabas, "Nonideal Analysis, Design and Voltage Mode Control of a Boost Converter", *57th International Scientific Conference, Power and Electrical Engineering of Riga Technical University (RTUCON)*, 13-14 Oct 2016, pp.1-6.